ISSN:2790-1688 DOI: 10.56028/aetr.1.1.207

Comparative Analysis on Two Severe Convective Processes in Hunan Province in 2020

Hui Zhou[1,2,a], Li Zhou[1,2,*], Ronghui Cai[1,2,b], Long Chen[1,2,c], Jia Tang[1,2,d], Minghui Tang[1,2,e]

[1] Hunan Meteorological Service, Changsha 410118, China
[2] author addresses Key Laboratory of Preventing and Reducing Meteorological Disaster in Hunan Province, Changsha 410118, China.

[a] 514446798@qq.com (H.Z.), [b] 54622813@qq.com (R.C.), [c] 393900092@qq.com (L.C.), [d] 156286532@qq.com (J.T.), [e] 3617176@qq.com (M.T.), [*] qiushui_wuhen@foxmail.com

Abstract. In this study, two severe convective weather processes in late March 2020 are compared and analyzed based on the surface observation data, Doppler weather radar data, satellite black body temperature data and the reanalysis data from the National Centers for Environmental Prediction. The results show that the two severe convective weather processes both can be divided into two stages, warm advection forcing stage and baroclinic frontogenesis stage. For the second process the warm advection forcing is not significant. In terms of dynamic conditions, in both processes there is low-level convergence, high-level divergence, middle-low-level southwesterly jet, and the intrusion of cold air. The upward motion in the second process is more intense than that in the first process. In both processes, the upward motion in the warm advection forcing stage is weaker than in the baroclinic frontogenesis stage. In the aspect of water vapor conditions, the divergence of water vapor flux at 850 hPa in the second process is larger than that in the first process. The water vapor convergence center rises to the level above 800 hPa and lasts for a long time. Through the comparative analysis in different stages, it is found that the water vapor convergence in the two processes in the baroclinic frontogenesis stage is stronger than that in the warm advection forcing stage. For the thermal conditions, the cold-dry air at high levels is superimposed over the warm-wet air at low levels, presenting a thermal unstable stratification. In the first process, the intensity and vertical extension of the low-level warm advection is larger than that in the second process. In both processes, the unstable energy is accumulated obviously in the warm advection forcing stage, and is released to a certain extent before the baroclinic frontogenesis stage. In the first process, there are 3 supercells within 100 km from ChangDe radar. In both processes, there are hails from 1900 BJT (Beijing Time) to 2000 BJT in Guanzhuang Town. The radar echoes both present the typical characteristics of hail. In the first process, the maximum reflectivity factor is larger, the intensity and vertical extension of mesocyclone are larger, the increase of vertical integrated liquid is more significant, and the high-level divergence is more intensive. Thus, the diameter of hail in the first process is larger.

Keywords: Severe convection; Water vapor; Unstable energy; Hail; Comparative analysis.

1. Introduction

With the rapid development of social economy and urbanization, the impact of local severe convective weather has become more and more serious, which has also attracted more and more attention [1-7]. Many scholars have conducted in-depth studies on severe convective weather from multiple angles, and analyzed various physical variables and radar echo characteristics of severe convective weather in detail. Luo et al. [8] analyzed a rare-seen intensive squall line process, and showed that there is obvious overhang echo, weak echo area, mesocyclone (mesovortex in the later maturity stage of squall line), strong rear inflow and the accompanied inflow gap in both the supercell stage and the squall line stage. such as. Ma et al. [9] studied and revealed the characteristics ambient parameters for extreme thunderstorm and gale events. Qiu et al. [10] studied the characteristics of physical variables for hail and short-term heavy precipitation events in Jiangsu, Shanghai and Zhejiang, and statistically analyzed the average differences of K index, precipitable water and wind shear.

ISSN:2790-1688 DOI: 10.56028/aetr.1.1.207

The spring and summer are the main seasons for severe convective weather in Hunan Province, which mainly includes thunderstorm, gale, hail and short-term heavy precipitation [11-15]. In recent years, several typical severe convective processes in Hunan Province have been diagnosed and analyzed. Cai et al. [16] studied 15 thunderstorm-gale processes, and summarized the synoptic situation, radar echo characteristics and the key point of forecast at different stages of the thunderstorm-gale processes. Yao et al. [17] analyzed a wide-range severe convective weather process in Hunan Province and found that there were significant adjustments on atmospheric circulation before the severe convection. The enhancement of the southwesterly low-level jet and the intrusion of cold-dry air in middle levels provided favorable environmental conditions for wide-range severe convection. Xu et al. [18] used a variety of statistical methods to analyze the variation trend of thunderstorm-gale events, and preliminary discussed the causes. They found that there are certain differences in the thermal unstable conditions in different areas.

In operational weather forecasts, severe convection is the difficult and key point. Compared with the researches on rainstorms caused by typhoon or Meiyu front, the researches on the prediction and early-warning of severe convection are not enough, which is difficult to meet the needs of short-term forecasting and nowcasting in operational weather forecasts. In late March 2020, two typical severe convection processes occurred in Hunan Province, accompanied by short-term heavy precipitation, hail and thunderstorm-gale. The hail diameter is large, and the wind speed of thunderstorm-gale is large and widely distributed. In this study, the two severe convection processes are compared and analyzed in detail. We hope the findings could deepen the understanding on the synoptic situation and physical variables of severe convective weather, and finally improve the prediction and early-warning of such disastrous weather.

2. Synoptic situation and disaster information

The first process was from March 21 to 22, 2020 referred as Process 1 in the following). The hails appeared at 20 counties in Hunan Province. The maximum diameter of hail was 6 cm, which appeared in Guanzhuang Town, Yuanling County, Huaihua City at 1900 BJT (Beijing Time) on March 21. There is thunderstorm-gale in 65 counties. The maximum wind speed reached 30.7 $m \cdot s^{-1}$ in Taojiang County, Yiyang City at 0200 BJT on March 22. The short-term heavy rainfall appeared in 252 counties. The maximum of hourly rainfall intensity was 83.2 mm, which appeared in Yongshun County, Xiangxizhou City at 0300 BJT on March 22 (Figs. 1a and 1b).

The second process was from March 26 to 27 (referred as Process 2 in the following). Hails occurred in 11 counties in Hunan Province. The maximum diameter of hail was 3 cm, which occurred in Yuanling County of Huaihua City and Xinhua County of Loudi City from 1900 BJT to 2200 BJT on March 26. Meanwhile, there were 48 counties with gales. The maximum wind speed was 25.4 $m \cdot s^{-1}$,, which appeared in Fengyushang of Yueyang City at 0100 BJT on March 27 (Figs. 1c and 1d). There were 372 counties with short-term heavy precipitation. The maximum of hourly rainfall intensity was 70.5 mm, which appeared in Xianrenyan forest farm, Chenxi County, Huaihua City.

ISSN:2790-1688
DOI: 10.56028/aetr.1.1.207

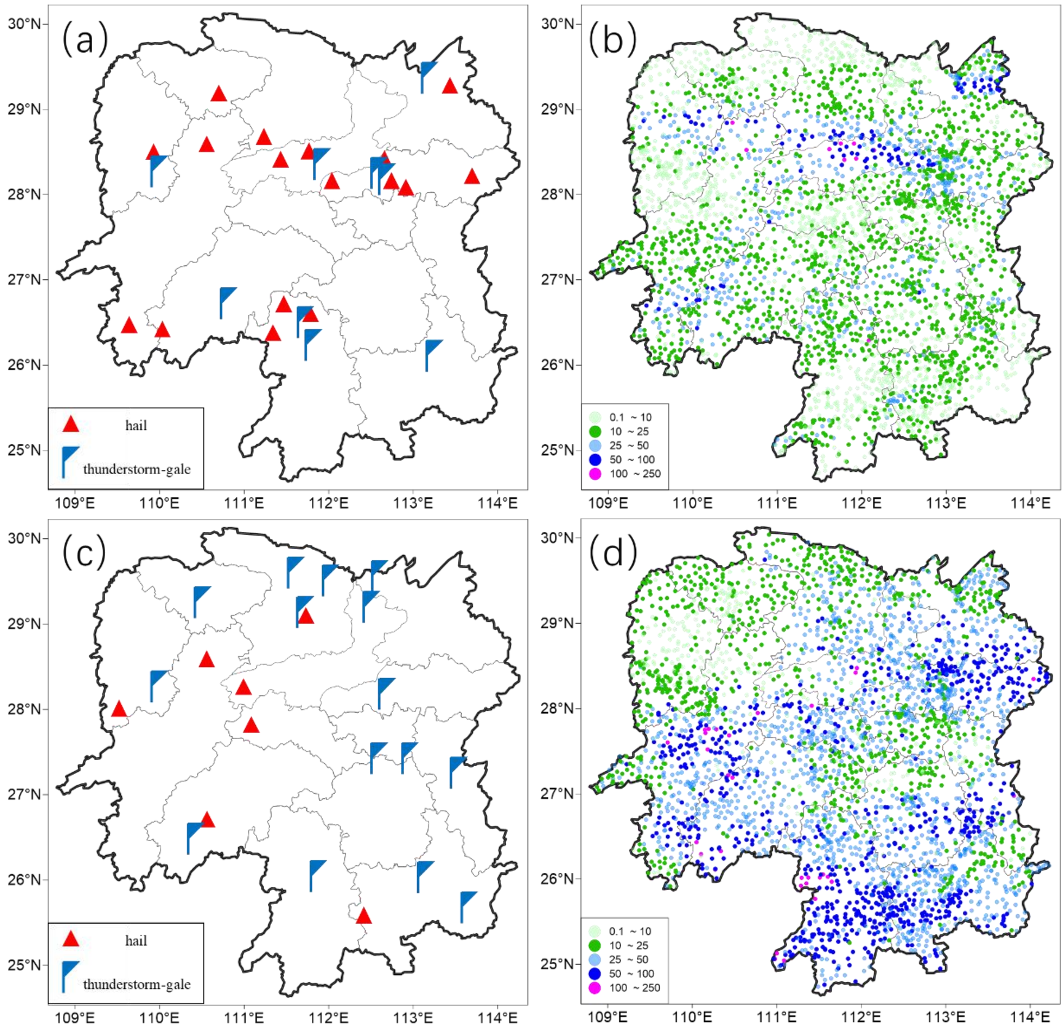

Figure 1. (a, c) Distributions of severe convection and (b, d) precipitation observation (mm) in Hunan Province. (a, b) Process 1; (c, d) Process 2.In both convective processes, there were hails, thunderstorm-gale and short-term heavy precipitation. Specifically, the disaster weather in Process 1 was mainly thunderstorm-gale and hail, while it was mainly short-term heavy precipitation in Process 2.

3. Characteristics of synoptic background

In Process 1, at 0800 BJT on March 21, Hunan Province was located on the right side of the entrance of high-level jet at 200 hPa (Fig. 2a), where there was positive vorticity and intensive divergence. At 500 hPa, there were two troughs and one ridge in the middle-high latitudes. Hunan Province was in front of the cold trough, where the positive vorticity advection is conducive to the convergence and uplift in the low levels. The southwest vortex at 850 hPa was located in the east of Sichuan. The warm shear in the eastern section of herringbone shear extended to the west of Human Province, and the wind shear reaches 18 m•s−1. The warm low pressure near the surface developed significantly. At 1700 BJT on March 21, there was a small low pressure generated along the convergence line, triggering the severe convective weather such as gale, hail and short-term heavy precipitation in western-northern Hunan Province. From the configuration of weather systems, the occurrence of severe convection at this stage belonged to the category of warm advection forcing proposed by Xu et al. [19-20].

At 2000 BJT on March 21, Hunan Province was located in front of the trough where there was positive vorticity advection, which was conducive to the convergence and upward movement in the low levels. Moreover, the forward-tilted trough provided favorable dynamic conditions for the occurrence of the second stage of convective weather. In terms of humidity conditions, the northern

ISSN:2790-1688 DOI: 10.56028/aetr.1.1.207
Hunan was dominated by the significant wet area at 850 hPa and dry tongue at 500 hPa. The unstable atmospheric stratification provided a beneficial condition for convective weather. The warm temperature ridge at 850 hPa converged with the cold shear at 700 hPa over western Hunan. At the same time, the cold air near the surface began to enter into Hunan Province from 2000 BJT on March 21. The convergence of cold and warm air promoted the enhancement and development of convection. The severe convection in this stage belongs to baroclinic frontogenesis convection.

In Process 2, at 2000 BJT on March 25 Hunan Province was located on the right side of the entrance of 200 hPa high-level jet where there was intensive divergence. There was a trough and a ridge in the middle and high latitudes at 500 hPa. There were warm and wet southwesterly airflow at both 700 hPa and 850 hPa over Hunan Province. From 2000 BJT on March 25 to 0500 BJT on March 26, there was a short convergence line on the north side of the Nanling Mountains moving rapidly eastwards and southwards along the mountains, resulting in a small-scale convective weather, which basically ended at 0800 BJT. Overall, the synoptic condition is this stage was not as favorable for severe convection as in Process 1. The convection in this stage of Process 2 was an atypical type forced by warm advection. According to Fig. 2d, at 2000 BJT on March 26, the low pressure trough at 500 hPa kept stable. The 850 hPa vortex was located over central Guizhou. The location of the warm shear in herringbone shear was close to that of the shear at 700 hPa, both located over the area from western Hunan to central Hunan. The convergence line at 925 hPa was located over southern Hunan Province. The area between the ultra-low shear line and mid-low shear line was the most unstable, which was conducive to the occurrence of convective weather such as short-term heavy precipitation. At 850 hPa, the wet area was wide, but 500 hPa was relatively dry. Hunan Province was under the control of unstable stratification. In addition, the cold air was strong, and the central pressure of cold high pressure reached 1027.5 hPa. The cold air quickly passed through Hunan Province and moved out at 1400 BJT on March 27. The convective weather in this stage was a typical type of baroclinic frontogenesis convection.

4. Characteristics of physical variables

4.1 Water vapor condition

Sufficient water vapor is very important for the occurrence of short-term heavy precipitation. Figure 2a shows the temporal cross-section of water vapor flux divergence and specific humidity in Hunan from March 21 to 23. It can be seen that during Process 1, the specific humidity maintained above 10 g•kg−1 at 850 hPa and reached 14 g•kg−1 near the surface, indicating that the humidity condition in the low levels is favorable for convection. The evolution of water vapor flux divergence shows that the water vapor converged obviously below 850 hPa from 0800 BJT on March 21 to 0800 BJT on March 23, especially from 1400 BJT on March 21 to 0800 BJT on March 22. There was a significant water vapor convergence center near 925 hPa, which was over northeastern Hunan Province with the central intensity above −15×10−5 g•s−1•cm−2•hPa−1. In this period, short-term heavy precipitation occurred.

Figure 2b shows the temporal cross-sections of water vapor flux divergence and specific humidity over Hunan Province from March 25 to 27. As can be seen, the specific humidity maintained above 10 g•kg−1 at 850 hPa and reached 14 g•kg−1 near the surface. The water vapor condition in the low levels is beneficial to the convective weather. The evolution of water vapor flux divergence exhibited that from 2000 BJT on March 25 to 1400 BJT on March 27, there was significant convergence of water vapor in the low levels below 800 hPa. Specially from 0800 BJT on March 26 to 1400 BJT on March 27, there was a significant water vapor convergence center near 850 hPa, which further moved southwards to southwestern Hunan Province with the central intensity exceeding −20×10−5 g•s−1•cm−2•hPa−1. This period is consistent with the occurrence period of short-term heavy precipitation in this severe convection process.

ISSN:2790-1688
DOI: 10.56028/aetr.1.1.207

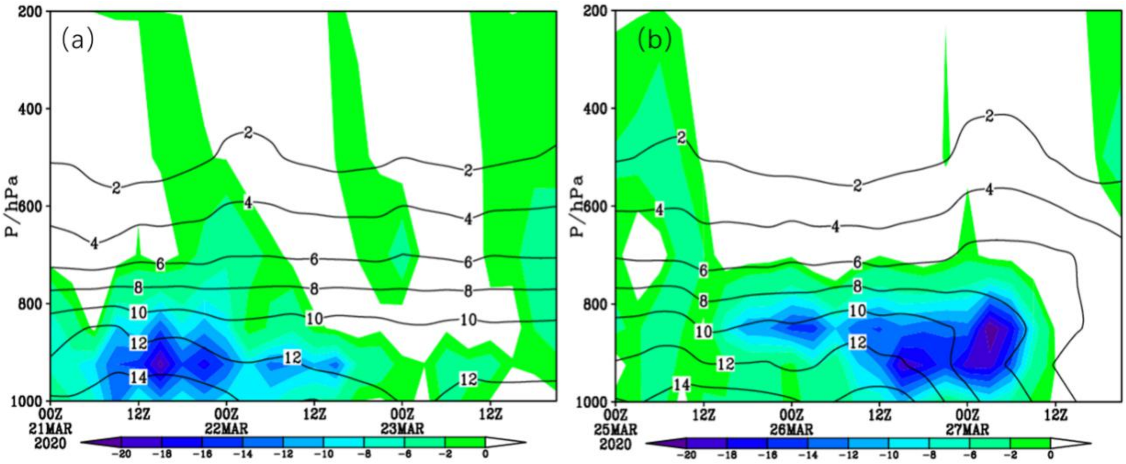

Figure 2. Temporal cross-sections of water vapor flux divergence (shaded, 10−5 g•s−1•cm−2•hPa−1) and specific humidity (contour, g•kg−1) over Hunan Province in the periods (a) from March 21 to 23 and (b) from March 25 to 27, 2020. The time in the abscissa is the Universal Time Coordinated (UTC).

To sum up, in both convective processes, the specific humidity maintained above 10 g•kg−1 at 850 hPa and reached 14 g•kg−1 near the surface. The water vapor flux divergence in Process 2 was larger than that in Process 1. The water vapor convergence center rose to the level above 800 hPa and lasted for a long time, indicating that the water vapor condition in Process 2 was better than in Process 2. Through the comparative analysis of different stages, it is found that the water vapor convergence of the two processes was more intense in the baroclinic frontogenesis stage than that in the warm advection forcing stage.

4.2 Dynamic conditions

The occurrence of severe convection must have favorable uplifting condition and initial disturbance. The upward motion is conducive to overcoming the convective inhibition energy. Figure 3 shows the cross-sections of vertical velocity and divergence of the two processes. It is found that from 0800 BJT on March 21 to 0800 BJT on March 23, there was a low-level convergence and high-level divergence, generating a strong upward motion. The strongest upward motion occurred at 0800 BJT on March 21 with the vertical velocity above 2×10−2 m•s−1, which was basically consistent with the occurrence period of the severe convection. From 0800 on March 26 to 2000 on March 27, there was also a low-level convergence and high-level divergence. The strongest upward motion occurred at 1100 BJT on March 27 with the vertical velocity exceeding 3×10−2 m•s−1. Therefore, the circulation configuration of high-level divergence and low-level convergence is conducive to the development of upward motion, providing a suitable triggering mechanism for severe convection.

Overall, in the aspect of dynamic conditions, there was low-level convergence and high-level divergence in both convective processes. The upward motion in Process 2 was stronger and maintained longer than in Process 1. According to the comparative analysis of different stages, it is revealed that in the two processes, the upward motion was weak in the warm advection forcing stage of both cases, and the dynamic conditions were more favorable in the baroclinic frontogenesis stage.

4.3 Thermal conditions

The favorable thermal conditions are necessary for severe convection, and they have a good indication of the intensity and duration of severe convective weather. Figure 4 shows the cross-sections of temperature advection along 113 °E in the most intensive development time of severe convection at 0200 BJT on March 22 and 0800 BJT on March 27. It can be seen that there was a deep warm advection area below 650 hPa over central Hunan at 0200 BJT on March 22 with the central intensity of 12×10−5 K•s−1. There was a cold advection area above 650 hPa over northern Hunan Province. The warm advection was the result of the intense development of low-level jet and ultra-low-level jet, which was conducive to the formation of warm-wet stratification in the middle-low levels. The high-level dry-cold stratification was superimposed over the low-level warm-wet stratification, resulting in the strong development of thermal instability. Under the trigger of upper-level pressure trough or near-surface convergence line, the thermal unstable energy can be released dramatically, promoting the occurrence of severe convective weather such as hail.

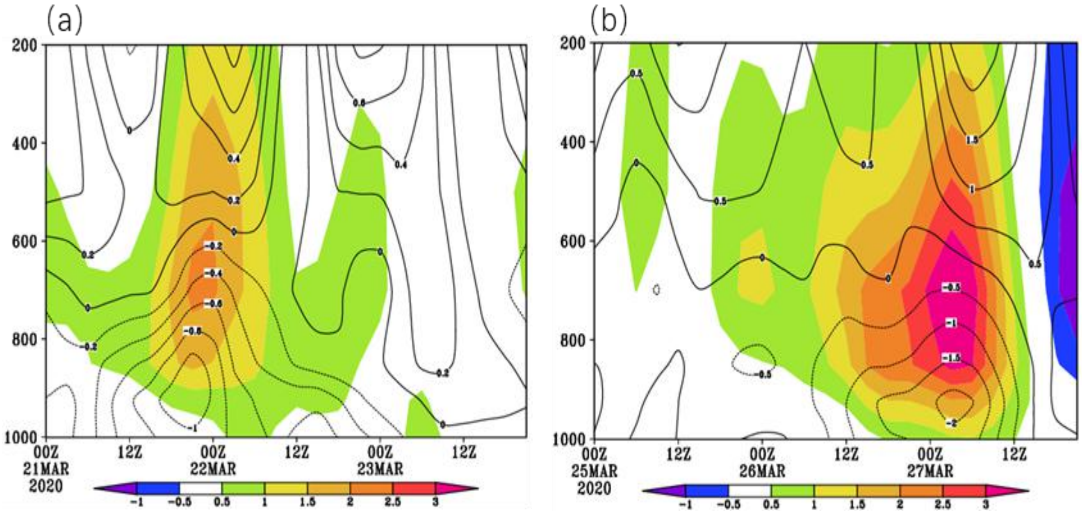

Figure 3. Temporal cross-sections of vertical velocity (shaded, 10−1 m•s−1) and divergence (contour, 10−5s−1) over Hunan Province in the periods (a) from March 21 to 23 and (b) from March 25 to 27, 2020. The time in the abscissa is UTC.

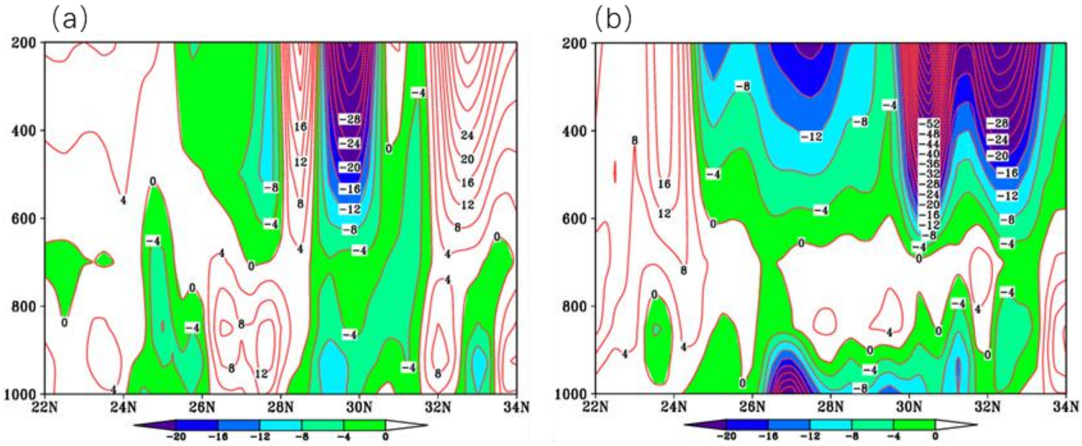

Figure 4. Cross-sections of temperature advection along 113 °E at (a) 0200 BJT on March 22 and (b) 0800 BJT on March 27 (10−5 K•s−1).

At 0800 BJT on March 27, there was also a warm advection area below 650 hPa over the north of central Hunan Province. The vertical extension was not as deep as that in Process 1 on March 22, and the intensity was also weak with the maximum value being 4×10−5 K•s−1. Above 650 hPa, the whole Hunan Province was basically controlled by cold advection, and the cold air was stronger than that on March 22. The weak low-level warm advection was covered by the strong high-level cold advection, resulting in the thermal instability stratification. Under the trigger of upper-level pressure trough or near-surface convergence line, the severe convective weather such as hail can occur.

In general, compared with Process 2, the intensity of warm advection was larger in Process 1 , the vertical extension of warm advection was deeper, and the cold air was weaker. Based on the

ISSN:2790-1688 DOI: 10.56028/aetr.1.1.207

comparative analysis of different stages, it is indicated that in the two processes, the accumulations of unstable energy in warm advection forcing stage were obvious, which were both released to a certain extent before the baroclinic frontogenesis stage.

5. Radar echo characteristics

5.1 Analysis on the radar echo characteristics in the first process

In Process 1, the supercell formed in the northwestern Hunan Province and then moved eastwards, which caused hail and thunderstorm-gale in several areas of northern Hunan, and short-term heavy precipitation in local areas. The hail intensively occurred in the period from 1830 BJT to 2300 BJT, which was in the warm advection forcing stage. There was a severe hail with a maximum diameter of 6 cm in Yuanling Town, Huaihua City. Analysis on radar echoes shows that there were three supercells within 100 km from ChangDe radar, and this phenomenon is rarely-seen. At 1937 BJT, there was a strong echo at low elevation with the maximum intensity above 65 dBZ. The three body scatter spike (TBSS) appeared at the elevation of 3.4° (Fig. 5a). The vertical integrated liquid (VIL) reached 70 kg•m−1. Figure 5b shows that there was a mesocyclone with the rotation speed reaching 20 m•s−1. Combined with the vertical profile of reflectivity factor (Fig. 5c), the strong echo above 50 dBZ extended up to 10 km, which was significantly higher than the height of −20°C and was conducive to the formation of hail. Meanwhile, the strong echo (≥60 dBZ) extended to surface, indicating that the hail landed. Moreover, the continuous favorable water vapor, unstable energy and upward movement conditions led to the continuous formation of new hail embryo. The hails were distributed almost in a line in the ground along the moving direction of the convective storm.

(a) (b) (c)

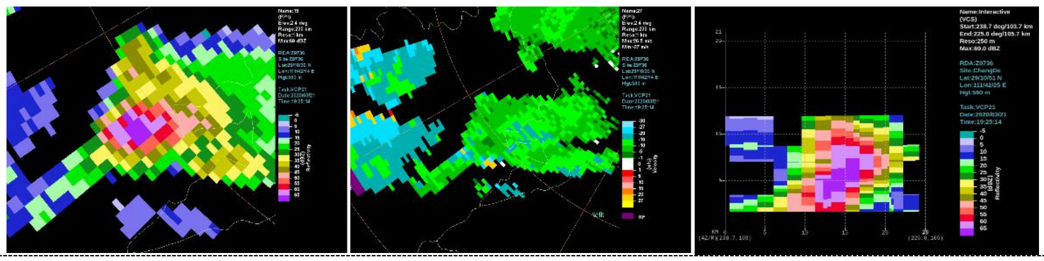

Figure 5. (a) Reflectivity factor at the elevation of 0.5° in Changde at 0203 BJT. (b) Radial velocity at the elevation of 1.5°. (c) Profile of reflectivity factor in Changde at 1925 BJT.

At 0200 BJT on March 21, the cold air moved southwards, affecting northern Hunan Province, and this time belonged to the baroclinic frontogenesis stage. The thunderstorm-gale in northern Hunan was caused by the intensive rotation of the mesocyclone in the supercell. At 0203 BJT, two supercells affected the Taojiang Town in Yiyang City, and the intensity in echo center was above 60 dBZ. There was significant TBSS at the elevation of 2.4° (Fig. 6a), which corresponded to the mesocyclone (with the rotation speed reaching 15 m•s−1) in western Taojiang Town in Fig. 6b. Figure 6c shows the attribute table of the storm cell causing the thunderstorm-gale in Taojiang Town. As can be seen, the predicted moving speed of the storm (the MVT product) reached 21 m•s−1.

The stations in Taojiang and Yongshun with large hourly rainfall intensity are selected for analysis. It is found that the maximum reflectivity factor of radar echo exceeded 60 dBZ due to the influence of supercell. There was intensive updraft in the front of the supercell, which was conducive to the occurrence of hail. The drag effect of the rear downdraft will also lead to thunderstorm-gale and short-term heavy precipitation. Affected by this supercell, the echo of 55 dBZ maintained for two volume-scans. Below 5 km, there was a precipitation echo of 45–55 dBZ with low centroid and high precipitation efficiency. Thus, the short-term heavy precipitation occurred in Lucidu Town, Taojiang County. Yongshun County was affected by a convective cell with strong echo intensity. The maximum intensity of the cell exceeded 60 dBZ, and new convective cells continuously generated in front of it. The convective cells continued to move eastward and then affected Yongshun County. The echo of 55 dBZ maintained for 4 volume-scans, leading to the short-term heavy precipitation in Yongshun.

(a) (b) (c)

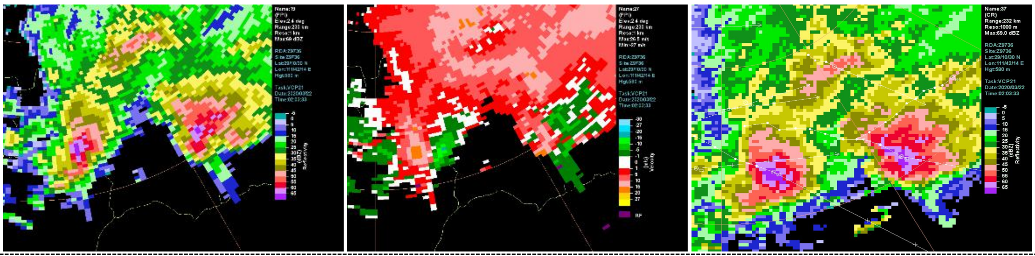

Figure 6. (a) Reflectivity factor at the elevation of 2.4° in Changde at 0203 BJT on March 21. (b) Radial velocity at the elevation of 1.5°. (c) Storm attribute table.

5.2 Analysis on the radar echo characteristics in the second process

The precipitation and severe convection in Process 2 can be divided into three stages. The first stage was from 2000 BST on March 25 to 1400 BST on March 26. The echoes affected southern Hunan Province from west to east, causing short-term heavy precipitation and local thunderstorm-gale. The second stage was from 1800 BST on March 26 to 0900 BST on March 27, when there was heavy rainfall and local hail. The third stage was from 10:00 BST on March 27 to 2300 BST on March 27. The low pressure trough in the middle level moved from west to east. The precipitation echoes moved eastwards and affected Hunan Province.

In this study, the radar echo characteristics in the first and second stages of Process 2are analyzed. The first stage was dominated by short-term heavy precipitation and gale. According to the analysis of echo characteristics of Yongzhou radar, there was a linear convection formed in the north of Yongzhou from 0400 BJT to 0600 BJT on March 26 with the maximum reflectivity factor of 60 dBZ (Fig. 7a). The echo with low centroid brought high-efficiency precipitation, and there was a “V” shaped weak echo area at the rear side (Fig. 7b). On the side with large echo gradient of the squall line, there was a high value area of low-level velocity. On the side along the echo moving direction, there was high-level divergence and downward momentum transmission in the middle-low levels. During this period, the wind speed in Shuangpai national station reached 16.4 m•s−1.

In the second stage, from 1920 BJT to 1940 BJT on March 26, there was heavy rainfall process accompanied with hail. The severe hail in Yuanling Town, Huaihua City had the diameter of 3 cm, which was a typical hail event caused by supercell storm. According to the analysis of the echo in Changde radar station (Figs. 8a and 8b), at 1902 BJT, the echo developed and the reflectivity factor of 55 dBZ expanded to about 8 km. At 1926 BJT, the maximum reflectivity factor reached 65 dBZ. The strong echo was overhanging. At the low-level echo area, there was obvious TBSS at the elevation of 3.4°. Moreover, there was obvious mesocyclone at the radial velocity diagram with the relative velocity of 18.5 m•s−1, reaching the medium intensity. By analyzing the storm attributes and the evolution of VIL, it is found that VIL increased significantly before hail occurred. From 0820 BJT to 1920 BJT, VIL reached 70 kg•m−2, which had increased by 30 kg•m−2. The maximum reflectivity factor reached 50 dBZ at 1844 BJT and extended to 6 km at 1856 BJT. The echo centroid reached 60 dBZ at 1914 BJT, the centroid height also extended to 6 km, and the echo top reached 11 km, which were conducive to the formation of large hail.

ISSN:2790-1688 DOI: 10.56028/aetr.1.1.207

(a) (b)

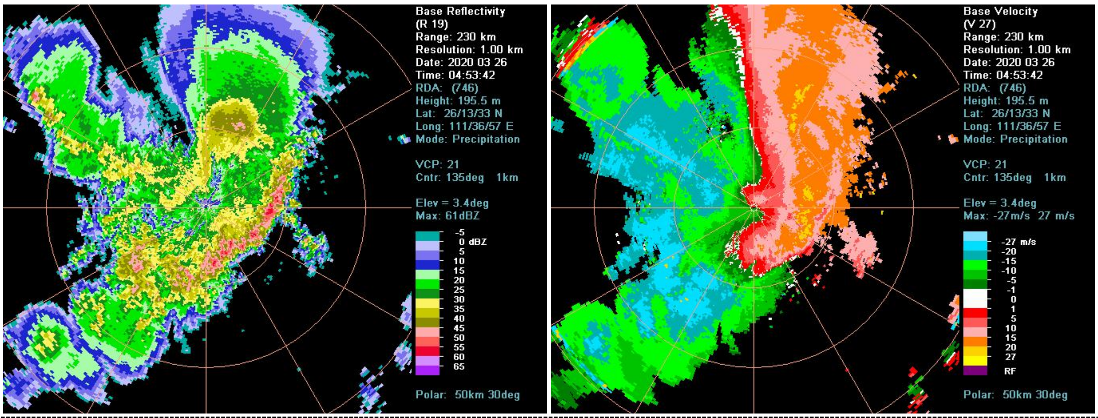

Figure 7. (a) Reflectivity factor at the elevation of 33° in Yongzhou at 0500 BJT on March 26. (b) Radial velocity at the elevation of 1.5°.

(a) (b)

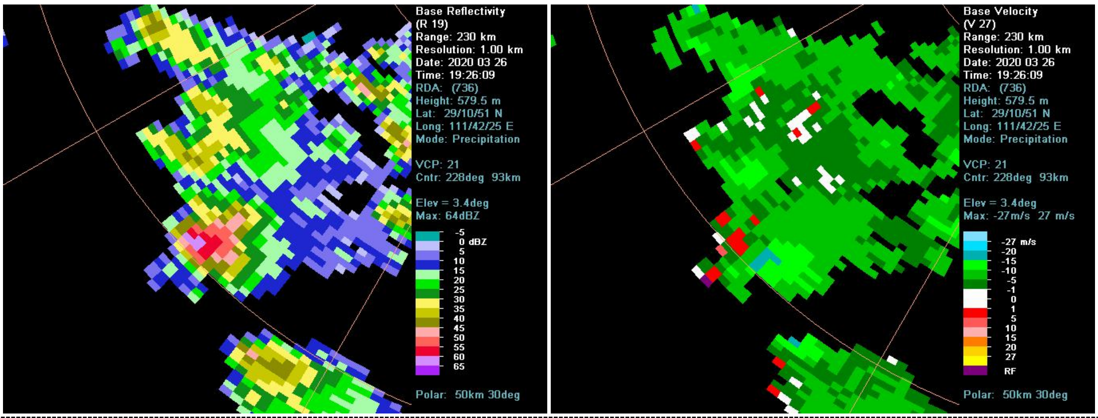

Figure 8. (a) Reflectivity factor and (b) radial velocity at the elevation of 3.4° in Changde at 1926 BJT on March 26.

5.3 Comparative analysis of the hail in Guanzhang Town in the two processes

In both processes, hail occurred from 1900 BJT to 2000 BJT in Guanzhuang Town, Huaihua City. The hail diameter was 6 cm in Process 1 and 3 cm in Process 2. From the analysis of the radar echo characteristics in Changde station (Table 1), it can be seen that the radar echoes presented typical hail echo characteristics in the two processes, such as the overhanging strong reflectivity factor, TBSS, weak echo region/bounded weak echo region, the sharp increase of VIL, strong mesocyclone, intensive high-level divergence and a high-altitude echo centroid (above 6 km). The maximum reflectivity factor in Process 1 (68 dBZ) was larger than that in the Process 2. In Process 1, the intensity of the mesocyclone was stronger, the VIL increase was larger, the mesocyclone extended to a higher altitude, and the high-level divergence was more intense. As a result, the hail in Process 1 was more severe than that in Process 2.

Compared with the radiosonde data at Changsha station (Fig. 9), the unstable energy of Process 1 was significantly larger. The convective available potential energy (CAPE) and downdraft convective available potential energy (DCAPE) reached 1928 J•kg−1 and 1210 J•kg−1, respectively, From the comparison of dynamic conditions (Table 2), it is found that the vertical wind shears at 0–3 km and 0–6 km in Process 1 were also significantly larger than those in Process 2. The larger vertical wind shear was conducive to the rapid development and organization of convective storms. Once the large unstable energy is released, it will cause more intense convective weather. In

ISSN:2790-1688 DOI: 10.56028/aetr.1.1.207

Process 1, the configuration of high-level dry air and low-level wet air was more obvious, and the precipitable water was relatively less. In Process 2, the wet layer was deep, and the precipitable water was up to 38 mm. Therefore, the disastrous weather was mainly hail and thunderstorm-gale in Process 1, and was mainly short-term heavy precipitation in Process 2.

Table 1. Comparison of echo characteristics of Changde radar between the two processes.

Time	2000 BJT on March 21	2000 BJT on March 26
Maximum reflectivity factor (dBZ)	68	65
Mesocyclone intensity ($m \cdot s^{-1}$)	20	18.5
Maximum VIL ($kg \cdot s^{-2}$)	72	65
TBSS	Yes	Yes
Maximum centroid height (km)	5	6
Maximum echo top height (km)	12	11
High-level divergence	Yes	Yes
Mid-altitude radial convergence	Yes	Yes
Weak echo region/ bounded weak echo region	Yes	Yes
Hail diameter (cm)	6	3

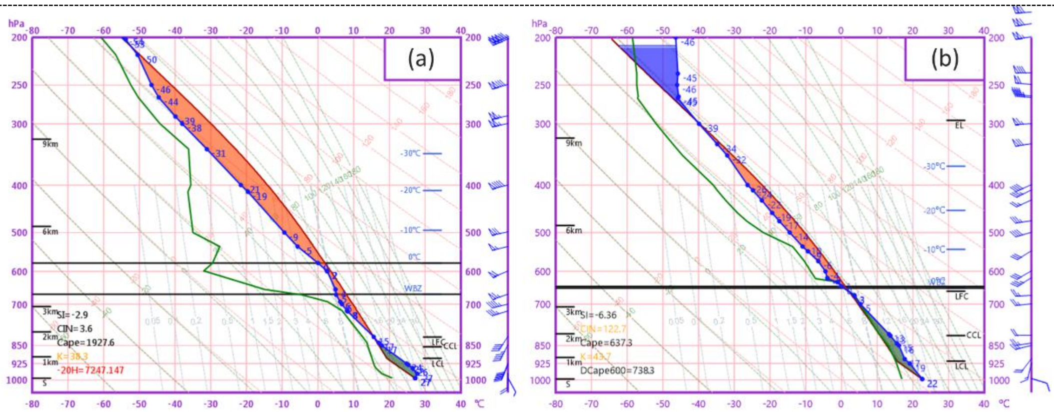

Figure 9. T-log P diagrams of Changsha radiosonde station at (a) 2000 BJT on March 21 and (b) 2000 BJT on March 26.

6. Conclusion

In this study, two severe convective weather processes in late March 2020 were compared and analyzed based on the surface observation data, Doppler weather radar data, satellite black body temperature data and the NCEP reanalysis data. The main results are as follows.

These two severe convective processes both can be divided into two stages, i.e. the warm advection forcing stage and the baroclinic frontogenesis stage. The main disastrous weather in the warm advection forcing stage of Process 1 was mainly thunderstorm-gale and hail, and that in Process 2 was mainly short-term heavy precipitation. The warm advection forcing in Process 2 was not significant.

In terms of dynamic conditions, the development of southwesterly jet in Process 1 was more intensive, but the cold air in Process was stronger. The upward motion of Process 2 over Hunan Province was more intense and persisted longer than that of Process 1. In these two processes, the upward motion in the warm advection forcing stage was weak, and the dynamic conditions in the baroclinic frontogenesis stage were more favorable for convection.

ISSN:2790-1688 DOI: 10.56028/aetr.1.1.207

Table 2. Comparison of physical variables at 2000 BJT between the two processes.

Time	2000 BJT on March 21	2000 BJT on March 26
Sur-CAPE (J•kg^{-1})	1928	637
DCAPE (J•kg^{-1})	1210	738
SI (°C)	-3	-6
LI (°C)	-5	-4
K (°C)	38	44
T850-500 (°C)	27	31
PWAT (mm)	35	38
Shear at 0–3 km (m•s^{-1})	18	13
Shear at 0–6 km (m•s^{-1})	29	17
WBZ layer height (m)	3523	3640
－20℃ layer height (m)	7247	6536

In terms of water vapor conditions, in both processes, the specific humidity was above 10 g•kg−1 at 850 hPa and 14 g•kg−1 near the surface. The water vapor flux convergence in Process 1 was larger than that in Process 2. In both processes, the water vapor convergence was stronger in the baroclinic frontogenesis stage than that in the warm advection forcing stage.

In terms of thermal conditions, the intensity of warm advection in Process 1 was stronger than that in Process 2, and the vertical extension was deeper. But the cold air was weaker in Process 2. The CAPE and K index also illustrated that the thermal conditions in Process 1 is more favorable for convection than in Process 2. In both processes, the accumulation of unstable energy in the warm advection forcing stage was obvious, but it was released to a certain extent before the baroclinic frontogenesis stage.

In Process 1, there were three supercells within 100 km, which was rarely seen. In both processes, there were hails from 1900 BJT to 2000 BJT in Guanzhuang Town, Yuanling County, Huaihua City with the hail diameters of 6 cm and 3 cm in Process 1 and Process 2, respectively. According to the analysis of radar echo in Changde station, the radar echoes both presented the typical characteristics of hail echo, such as the overhanging strong reflectivity factor, TBSS, weak echo region/bounded weak echo region, the sharp increase of VIL, strong mesocyclone and intensive high-level divergence. In Process 1, the maximum reflectivity factor was larger, reaching 68 dBZ, the intensity of mesocyclone was larger, the sharp increase of VIL is more significant, the vertical extension of mesocyclone was deeper, and the high-level divergence was more intensive. Thus, the disastrous weather in Process 1 was more severe, and the diameter of hail was larger.

Author Contributions: Conceptualization, Zhou H. and Zhou L.; methodology, Zhou L. and Cai R.H.; validation, Chen L. and Tang J.; formal analysis, Zhou H. and Tang M.H.; data curation, Zhou L. and Chen L.; writing—original draft preparation, Zhou L. and Cai R.H.; writing—review and editing, Zhou H. and Zhou H.; project administration, Zhou L. All authors have read and agreed to the published version of the manuscript.

Acknowledgments

The research in this paper is supported by the Innovation and Development Program of China Mete-orological Administration (grant number CXFZ2021J020), and Hunan Research and Development Program of Key Fields (grant number 2019SK2161).

Reference

[1] Xu, R.; Miao, J.F.; Tan, Z.M. Numerical Simulation of the Impact of Urban Underlying Surface Characteristics on Thunderstorm in Nanjing. Chinese Journal of Atmospheric Sciences. 2013, 37(6): 1235-1246. DOI：10.3878/j.issn.1006-9895.2012.12128. (In Chinese)

[2] Li,G.L.; Li J.; Li, X.; et al. The Feature Analysis of the Strong Thunderstorm Weather Forecast on August 30 in Hubei Province. Hubei Agricultural Science. 2018, 57(16):35-38. DOI：CNKI:SUN:HBNY.0.2018-16-008. (In Chinese)

[3] Su, T.; Miao, J.F.; Wang, Y.H. Impact of radiative transfer parameterizations on simulated sea breeze thunderstorm over the Hainan Island. Chinese Journal of Geophysics. 2017, 60(8): 3023-3040. DOI：CNKI:SUN:DQWX.0.2017-08-011. (In Chinese)

[4] Duan, X.; Li, Y. Diagnostic Analysis of Moist Potential Vorticity for heavy rain in Middle Yunnnan . Plateau Meteorology. 2000, 19(2): 253-259. DOI：10.3321/j.issn:1000-0534.2000.02.014. (In Chinese)

[5] Gao, S.; Lei, T.; Zhou, Y.S. Diagnostic analysis of moist potential vorticity anomaly in torrential rain systems. J Appl Meteor Sci. 2002, 13(6): 662-670. DOI：10.3969/j.issn.1001-7313.2002.06.003. (In Chinese)

[6] Zhang, D.M. Comparative Analysis of Two Hail Processes Based on Doppler Weather Radar Products in Fuxin City in 2009. HUBEI AGRICULTURAL SCIENCES. 2018, 57(7): 48-53. DOI：CNKI:SUN:HBNY.0.2018-07-011. (In Chinese)

[7] Zhang, C.L.; Lou, F.l.; Zhou, F.R. The Northeast Cold Turbo-induced A Strong Winds, Precipitation,Hail Weather Process Analysis. HUBEI AGRICULTURAL SCIENCES. 2018, 57(4): 39-43. DOI：10.14088/j.cnki.issn0439-8114.2018.04.010. (In Chinese)

[8] Luo, Q.; Zhang, Y.G.; Cheng, M. Evolution and Development Mechanisms of a Rare Strong Arc-shaped Squall Line Occurring in Northern Beijing in 2017. Acta Meteorological Sinica. 2019,77(3): 371-386. DOI：CNKI:SUN:QXXB.0.2019-03-001. (In Chinese)

[9] Ma, S.P.; Wang, X.M.; Yu, X.D. Environmental parameter characteristics of severe wind with extreme thunderstorm. J Appl Meteor Sci. 2019, 30(3): 292-301. DOI:CNKI:SUN:YYQX.0.2019-03-004. (In Chinese)

[10] Qiu, J.J.; He, L.F. Comparative Analysis on Weather Characteristics and Convective Parameters of Torrential Rain and Hail in Yangtze River Delta. Meteor Mon. 2013, 39(5):577-584. DOI:10.7519/j.issn.1000-0526.2013.05.005. (In Chinese)

[11] XU, L.; Yao, R.; Li, Q.Y. et al. Comparison on Two Continuous Rainstorms in Midsummer in Hunan Province. Journal of Meteorology and Environment. 2015, 31(3): 15-22. DOI:10.3969/j.issn.1673-503X.2015.03.003 . (In Chinese)

[12] Ye, C.Z.; Pan, Z.X.; Liu, Z.X.; et al. Mechanism triggering the '03.7' heavy rainfall in the northwest of Hunan Province. J Appl Meteor Sci. 2007, 18(4): 468-478. DOI:10.11898/1001-7313.20070407. (In Chinese)

[13] Mao, Do.Y.; Zhou, Y.H.; Zhang, F.H. et al.Mesoscale Analysis of Flash Flood in Early Summer of 2005 in Hunan. Meteor Mon. 2006, 32(3):63-70. DOI:10.7519/j.issn.1000-0526.2006.3.011 . (In Chinese)

[14] Zhou, H.; Cai, R.H.; Ying, D.D.; et al. Causes Analysis of an Extreme Persistent Rainstrom in Hunan Province in July 2016. Journal of Arid Meteorology. 2018, 36(1): 56-63. DOI:10.11755/j.issn.1006-7639(2018)-01-0056. (In Chinese)

[15] Li, F.; Zhang, F.H.; Xiong, M.Q.; et al. Environment Field and Maintaining Mechanism Analysis of “5.31” Heavy Rainfall in Hunan in 2005. Meteor Mon. 2006, 32(3):71-77. DOI:10.7519/j.issn.1000-0526.2006.3.012. (In Chinese)

[16] Cai, R.H.; Yao, R.; Huang, X.Y.; et al. Synoptic Situation Classification and Forecast Analysis of Thunderstorm in Dongting Lake. Meteor Mon. 2017, 43(5): 560-572. DOI:10.7519/j.issn.1000-0526.2017.05.005. (In Chinese)

[17] Yao, R.; Tang, J.; Lan, M.C.; et al. Analysis of the environment condition and evolution characteristic for a mixture strong convective event. Torrential Rain and Disasters. 2017, 36(03): 217-226. DOI:10.7519/j.issn.1000-0526.2017.05.005. (In Chinese)

[18] Xu, L.; Yao, R.; Wang, X.L.; et al. Study of Temporal-Spatial Distribution and Variation Characteristics of Thunderstorm Gales in Hunan. Plateau Meteorology. 2017, 36(4): 993-1000. DOI：10.7522/j.issn.1000-0534.2016.00088. (In Chinese)

ISSN:2790-1688 DOI: 10.56028/aetr.1.1.207

[19] Xu, A.H.; Sun, J.S.; Xu, D.B.; et al. Basic Synoptic Situation Classification and Element Character of Severe Convection in China. Meteor Mon. 2014, 40(4): 400-411. DOI:CNKI:SUN:QXXX.0.2014-04-002. (In Chinese)

[20] Tang, M.H.; Wang, Q.; Xu, J.Y.; et al. Comparative analysis of two squall line events under low-level warm convection forcing in Hunan. Torrential Rain and Disasters. 2019, 38(2): 115-125. DOI： CNKI:SUN:HBQX.0.2019-02-003. (In Chinese)